Well-Defined Ti Surface Sites in Ziegler-Natta Pre-Catalysts from 47/49Ti solid-state Nuclear Magnetic Resonance Spectroscopy

Alexander V Yakimov, Christoph J Kaul, Yuya Kakiuchi, Sebastian Sabisch, Felipe Morais Bolner, Jean Raynaud, Vincent Monteil, Pierrick Berruyer, Christophe Copéret

▶ **To cite this version:**

Alexander V Yakimov, Christoph J Kaul, Yuya Kakiuchi, Sebastian Sabisch, Felipe Morais Bolner, et al.. Well-Defined Ti Surface Sites in Ziegler-Natta Pre-Catalysts from 47/49Ti solid-state Nuclear Magnetic Resonance Spectroscopy. 2023. hal-04296050

HAL Id: hal-04296050
https://hal.science/hal-04296050

Preprint submitted on 20 Nov 2023

HAL is a multi-disciplinary open access archive for the deposit and dissemination of scientific research documents, whether they are published or not. The documents may come from teaching and research institutions in France or abroad, or from public or private research centers.

L'archive ouverte pluridisciplinaire **HAL**, est destinée au dépôt et à la diffusion de documents scientifiques de niveau recherche, publiés ou non, émanant des établissements d'enseignement et de recherche français ou étrangers, des laboratoires publics ou privés.

Well-Defined Ti Surface Sites in Ziegler-Natta Pre-Catalysts from $^{47/49}$Ti solid-state Nuclear Magnetic Resonance Spectroscopy

Alexander V. Yakimov[a,‡,*], Christoph J. Kaul[a,‡], Yuya Kakiuchi[a], Sebastian Sabisch[a], Felipe Morais Bolner[b], Jean Raynaud[b], Vincent Monteil[b], Pierrick Berruyer[c], Christophe Copéret[a,*]

[a] Department of Chemistry and Applied Biosciences, Laboratory of Inorganic Chemistry, Surface & Interfacial Chemistry, Eidgenössische Technische Hochschule Zürich, HCI, Vladimir-Prelog-Weg 2, CH-8093 Zurich, Switzerland

[b] Université de Lyon, CNRS, Université Lyon 1, CPE Lyon, UMR 5128 - CP2M (Catalysis, Polymerization, Processes & Materials), PolyCatMat team, 69616 Villeurbanne, France

[c] Institut des Sciences et Ingenierie Chimiques, École Polytechnique Fedérale de Lausanne (EPFL), CH-1015, Lausanne, Switzerland

KEYWORDS. Ziegler-Natta catalysts, solid-state NMR, DFT calculations, High-field $^{47/49}$Ti NMR.

ABSTRACT: Ziegler-Natta (ZN) catalysts – typically formulated as $TiCl_4/MgCl_2/AlR_3$ and possibly containing additional organic ligands – are essential to the production of polyethylene and polypropylene. Despite their industrial relevance and years of research on these materials, the role of each constituent (support, organic ligands, post-treatment with organic or inorganic modifiers *etc.*) on the structure of Ti surface sites responsible for polymerization remains poorly understood, partly because of the high complexity of such materials. Herein, we show how high-field $^{47/49}$Ti NMR can bring about new lights on the structures of the Ti surface sites in ZN pre-catalysts (prior to activation with alkyl aluminium) resulting from adsorption of $TiCl_4$ on $MgCl_2$ followed by a post-treatment with BCl_3, an additive used to improve catalytic activity by increasing the amounts of active sites. The implementation of high-field NMR (900 MHz), low temperature (~100 K), magic angle spinning (10 kHz), CPMG echo train acquisition and DFT modelling, to study this material ($TiCl_4/MgCl_2/BCl_3$) and molecular analogs, allows the detection of a $^{47/49}$Ti NMR signature and the development of a molecular level understanding of the NMR signature of Ti surface sites. The extracted ^{49}Ti NMR parameters ($\delta_{iso,\,exp}$ = −170 ppm and $C_{Q,\,exp}$ = 9.3 MHz) from this signature analyzed by DFT modeling indicate the presence of one specific coordination sphere for Ti, namely a fully chlorinated hexacoordinated Ti site with a symmetric charge distribution, due to the post-treatment with BCl_3 (that removes the alkoxide ligands) and the coordination environment provided by surface of an amorphous $MgCl_2$.

Introduction

Heterogeneous Ziegler-Natta (ZN) catalysts[1-3] are central for the industrial production of polyethylene (PE grades such as HDPE & LLDPE) and polypropylene (PP such as *iso*PP).[4] These catalysts are multicomponent hybrid materials that include organic (ether, alcohol and esters, referred to as internal donors) and inorganic parts ($TiCl_4/MgCl_2$),[5] which are activated with alkyl aluminum, e.g. $Al(C_2H_5)_3$, in the presence or not of additional organic promoters (external donors), to provide polymers with specific properties resulting from the molar masses, the dispersity and the stereoselectivity when applicable (*iso*PP).[6] Despite intensive studies over the past decades,[7-16] establishing structure–activity relationships in ZN catalysts has remained elusive. The situation is particularly challenging because of the low Ti weight loading (2-4 wt. %), and the multistep catalyst preparation, where the state of Ti sites and the structure of the $MgCl_2$ support undergoes changes at every stage. This process ultimately results in a small fraction of catalytically active Ti sites upon activation with alkyl aluminum reagents.[17]

EPR spectroscopy combined with DFT modeling has recently enabled to identify the spectroscopic signature of Ti active sites in activated ZN PE catalysts and to assign them to a specific structural motif, namely a bimetallic Ti(III)/Al alkyl species.[17] Despite these advances, establishing a link between the Ti site structures before and after activation remains an important question in order to establish the role of $MgCl_2$ on the structure of the surface sites and a detailed structure-activity relationship. While the preparational procedure of $MgCl_2$ is known to be critical to generate highly active catalysts,[18] understanding the interaction of Ti with the support surface is complicated because $MgCl_2$ loses crystallinity upon interaction with $TiCl_4$.[19] Thus, structural investigations based on XRD or other techniques that rely on long-range order, are not that informative. While optical spectroscopy (IR, UV-Vis, Raman, etc.)[14], XAS techniques[20] and various multinuclear NMR (^{1}H, ^{13}C, ^{25}Mg, and ^{35}Cl)[21-25] methods have been successfully used for addressing the structure of Ti sites on $MgCl_2$, the results are very difficult to interpret and lead to rather poor molecular-level understanding. Furthermore, previous studies have also shown that the internal donors such as THF or ethanol, that are known to activate $MgCl_2$, are non-innocent and react with $TiCl_4$ resulting in the formation of surface Ti alkoxide species,[26, 27] that may explain the broad range of reactivity of surface sites. In fact, the addition of BCl_3 (and other MCl_x additives) has been proposed to remove surface alkoxy species *via* transmetallation

https://doi.org/10.26434/chemrxiv-2023-2hmzj-v2 **ORCID:** https://orcid.org/0000-0002-8624-1002 Content not peer-reviewed by ChemRxiv. **License:** CC BY-NC-ND 4.0

by forming B-alkoxide species. Note that this treatment also results in a significant removal of Ti sites (see Table S2 for elemental analysis), while increasing the number of active sites when the pre-catalyst is treated with triethylaluminum (TEA).[17, 26-28]

Thus, resolving the structure of Ti surface sites formed upon adsorption of $TiCl_4$ on activated $MgCl_2$ is still of prime interest and calls for the development of characterization techniques, that can probe the local environment and electronic structure of the Ti sites. Considering that these sites are Ti(IV) and diamagnetic, $^{47/49}$Ti NMR appears to be a perfect candidate. However, $^{47/49}$Ti NMR spectroscopy suffers from a number of critical limitations, namely i) the low gyromagnetic ratio of both ^{49}Ti and ^{47}Ti nuclei, ii) the low natural abundance of these nuclei (5.41 and 7.44 % correspondingly), iii) the quadrupolar nature of the nuclei (I = 7/2 and 5/2, respectively), iv) the rather large quadrupole moment of both nuclei (24.7 and 30.2 fm^2, correspondingly),[29] and v) close proximity of these isotopes in the NMR spectra (within 267 ppm), often yielding overlapping broad lines.[30] All these factors contribute to the difficulty in obtaining high quality $^{47/49}$Ti NMR spectra, usually associated with a poor signal-to-noise ratio and complex line shapes. The situation is further worsened for ZN catalysts due to the low amount of Ti (often about 2-4 wt. % in range), the expected heterogeneity of surface sites formed upon the adsorption of $TiCl_4$ on specific sites of $MgCl_2$ as well as the presence of Ti with both Cl and OR ligands.[26, 27] Pioneering work on $^{47/49}$Ti NMR of Ziegler-Natta pre-catalysts led to observation of a very broad low-intense signal, which is difficult to interpret.[31] However, recent hardware developments (higher fields, low temperature) augmented with computational approaches have shown that it is possible to detect the NMR signature of Ti sites in Ti silicalite (TS-1), another industrially relevant materials containing only 1-2 wt% Ti.[32]

A specific challenge associated with the characterization of the ZN catalyst is $MgCl_2$ itself. Its disordered character (upon adsorption of $TiCl_4$)[19] makes the development of meaningful DFT models particularly challenging, due to the lack of the corresponding crystal structure. Consequently, previously Ti surface models used for DFT computations were based on $TiCl_4$ adsorbed on various facets of crystalline $MgCl_2$.[31] However, recent findings related to the characterization of the corresponding V-based ZN pre-catalysts (prepared by adsorption of $VOCl_3$ on similar $MgCl_2$) have shed light on how the morphology of $MgCl_2$ can affect the structure of the V sites and the NMR signatures, thanks to the high sensitivity of ^{51}V NMR combined with computations.[33] Namely, adsorption of $VOCl_3$ on $MgCl_2$-$(THF)_{1.5}$ generates a well-defined V-alkoxide surface species, with a distorted local geometry due to loss of crystallinity of $MgCl_2$.[33] Encouraged by the advances in solid-state NMR and computational modeling, along with our improved understanding of $MgCl_2$ and its impact on the local geometry of surface sites, we investigate here the corresponding Ti-based ZN PE pre-catalysts by combining high magnetic field (900 MHz), magic angle spinning (MAS), low temperature (~100 K), higher filling factor (3.2 mm thin-wall rotor, ~40 µL sample volume), and probe optimized for low-gamma nuclei, with DFT computations benchmarked on molecular compounds. This multipronged approach unveils the structure of Ti sites in ZN PE catalysts, prepared from the adsorption of $TiCl_4$ on $MgCl_2$ followed by a BCl_3 treatment.[28]

Results and discussions

NMR measurements

We first conducted $^{47/49}$Ti NMR measurements on two molecular complexes in order to assess the effect on NMR signatures of specific Ti local environments, representative of possible surface sites, namely $[H_2NMe_2]_2[TiCl_6]$[34] and $[H_2NMe_2]_2[TiCl_5(O^iPr)]$. For the NMR measurements, the Double Frequency Sweep – Quadrupolar Carr-Parcell-Meiboom-Gill (DFS-QCPMG) methodology was selected in order to gain from DFS (signal enhancement), MAS (narrowing down NMR line) and CPMG (signal enhancement by echo train acquisition).[35, 36]

While $[H_2NMe_2]_2[TiCl_6]$ shows two relatively narrow lines (<1 kHz) corresponding to the ^{49}Ti and the ^{47}Ti isotopes (Fig. 1a), the Ti complex having one alkoxide ligand does not show any NMR signal under similar conditions, likely due to a too large quadrupolar coupling constant associated with a much larger asymmetric environment (*vide infra*). Fitting the spectrum for $[H_2NMe_2]_2[TiCl_6]$ yields a $C_Q(^{49}Ti)$ = 3.0 MHz, $\delta_{iso}(^{49}Ti)$ = −250 ppm.

On the basis of the narrow lines, this sample was used for the calibration of NMR measurement parameters, which was of highest importance for the spectra of ZN pre-catalysts. We next focused on ZN catalysts ($TiCl_4$@$MgCl_2(THF)_{1.5}$) treated with BCl_3, in order to remove possible alkoxide ligands and increase our chances to obtain an NMR spectrum with narrower lines (*vide infra*), a highly active in ethylene polymerization (see ESI Fig. S2). The $^{47/49}$Ti DFS-QCPMG NMR spectrum of BCl_3-treated sample shows only a broad feature centred at ca. -276 ppm with a number of sidebands (Fig. 1b), whose peak position and width is consistent with a surface Ti site in a similar Ti coordination environment as in $[H_2NMe_2]_2[TiCl_6]$. The signal can be fitted to a single Ti site (with both ^{49}Ti and ^{47}Ti isotopes; we note that due to larger electric quadrupolar moment ^{47}Ti isotope leads to a very broad line on a level of background) with a $\delta_{iso}(^{49}Ti)$ of −170 ppm and a $C_Q(^{49}Ti)$ of 9.3 MHz, which indicate that Ti is in a distorted octahedral environment with likely only Cl ligands. Notably, no $^{47/49}$Ti NMR signal could be obtained on the pristine sample (without prior treatment with BCl_3) consistent with what we observe for the molecular compound and as expected for Ti sites having large C_Q due to the presence of both Cl and OR ligands as revealed by ^{13}C MAS NMR (see ESI Fig. S3 for details).

https://doi.org/10.26434/chemrxiv-2023-2hmzj-v2 **ORCID:** https://orcid.org/0000-0002-8624-1002 Content not peer-reviewed by ChemRxiv. **License:** CC BY-NC-ND 4.0

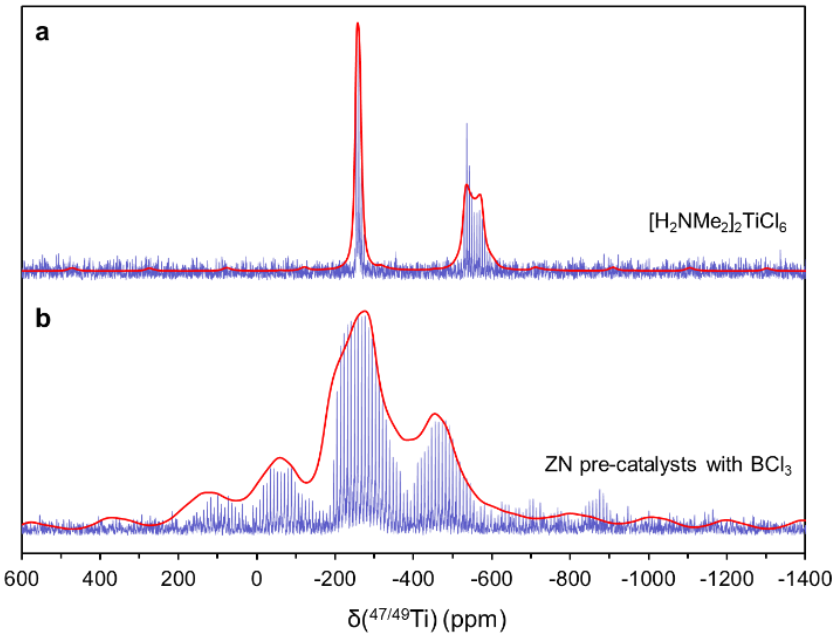

FIGURE 1. $^{47/49}$Ti DFS-QCPMG MAS NMR spectra (10 kHz MAS, 21.1 T, 100 K) for (a) $[H_2NMe_2]_2[TiCl_6]$ (512 scans) and (b) ZN pre-catalyst treated with BCl_3 (370'496 scans) as well as modeled line shape (solid red line) for δ_{iso} = -170 ppm and C_Q = 9.3 MHz. Magnitude correction was used for the representation.

TABLE 1. Calculated ^{49}Ti NMR spectroscopic signatures (δ_{iso} / ppm, C_Q / MHz) of model Ti surface species in ZN pre-catalysts

Adsorbate	Model					
$TiCl_{4-x}(OR)_x$[a]	$[TiCl_{6-x}(OR)_x]^{2-}$		$TiCl_{4-x}(OR)_x$ @$MgCl_2$-110		$TiCl_{4-x}(OR)_x$ @$MgCl_2$-NR	
	δ_{iso}	C_Q	δ_{iso}	C_Q	δ_{iso}	C_Q
$TiCl_4$	-203	2.1	-64	15.3	-122	11.7
$TiCl_3OR$	-573	37.9	-489	27.5	-511	33.8
$TiCl_2(OR)_2$	-	-	-763	30.4	-760	33.7

[a]x = 0, 1 or 2

DFT calculations

In this study, we investigated the contributions that affect the NMR signatures – namely the chemical shift anisotropy and C_Q – of molecular model systems as well as model surface species. For this purpose, we conducted DFT calculations of the NMR parameters[37] – using B3LYP,[38, 39] QZ4P,[40] and the all electron scalar relativistic zeroth-order regular approximation (ZORA)[41] – to explore these contributions. For the purpose of benchmarking the computational protocol, we used a library of molecular compounds with previously reported solution $^{47/49}$Ti NMR isotopic chemical shifts and observed a good agreement between computation and experiment (referenced against benchmark correlation, see ESI for details).[42-44] Building on this DFT protocol, the NMR calculations based on the crystal structures of the molecular compounds $[H_2NMe_2]_2[TiCl_6]$ and $[H_2NMe_2]_2[TiCl_5(O^iPr)]$, confirmed a very high sensitivity of the chemical shift and C_Q towards substitution between chlorido and alkoxide ligands. Having one alkoxide ligand is enough to decrease the chemical shift from -203 ppm to -573 ppm, but also to induce a significant increase in the C_Q from 2.1 to 37.9 MHz when compared to the hexachlorido compound, $[H_2NMe_2]_2[TiCl_6]$. Consequently, the lineshape of the Ti-alkoxy species is expected to be significantly broadened compared to the highly symmetric $[H_2NMe_2]_2[TiCl_6]$ species, thus explaining the difficulty to observe and the absence of $^{47/49}$Ti NMR signal for $[H_2NMe_2]_2[TiCl_5(O^iPr)]$ and the related supported ZN catalysts prior to treatment with BCl_3 under our experimental conditions.[26, 27]

Next, the ^{49}Ti NMR signatures of model ZN surface sites were investigated as shown in Table 1, inspecting the effect of directly bound ligands (Cl vs. OR) as well as the $MgCl_2$ morphology, focusing on the difference between the representative crystalline (110)-facet ($TiCl_{4-x}(OR)_x$@$MgCl_2$-110) vs. an disordered environment around Ti/Mg modeled by a nanoribbon structure ($TiCl_{4-x}(OR)_x$ @$MgCl_2$-NR).[33] The calculated ^{49}Ti NMR signatures for the models built from the commonly employed crystalline $MgCl_2$ (110)-facet surface[21, 22, 45-49] show a similar trend as the molecular model systems discussed above: the chemical shift decreases upon introduction of terminal alkoxide ligands from –64 ppm for the fully chlorinated titanium ($TiCl_4$@$MgCl_2$-110)

https://doi.org/10.26434/chemrxiv-2023-2hmzj-v2 **ORCID:** https://orcid.org/0000-0002-8624-1002 Content not peer-reviewed by ChemRxiv. **License:** CC BY-NC-ND 4.0

to –489 and –763 ppm for the mono- and bis-alkoxide systems, respectively. This is accompanied by a significant increase in C_Q from 15.3 MHz for the perchlorinated species to 27.5 MHz and 30.4 MHz for the mono- or bis-alkoxide model surface sites.

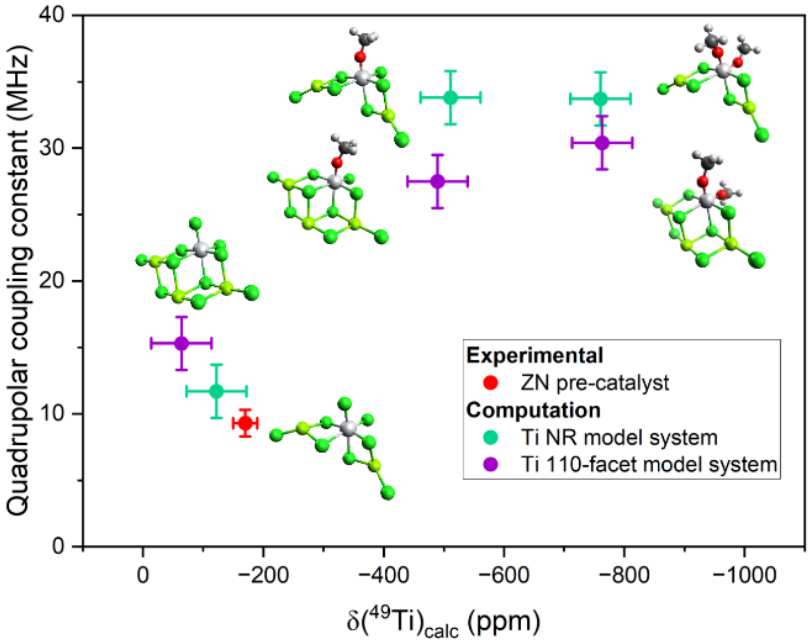

FIGURE 2. Two-dimensional map of calculated ^{49}Ti NMR signatures for the nanoribbon (green points) and (110)-facet model systems (violet points). Experimental value of BCl_3-treated ZN pre-catalysts (red point). The deviations from the computed values were estimated from the benchmark sets for the chemical shift (ca. ±50 ppm) and C_Q (ca. ±2 MHz).

Although, the trend of the isotropic chemical shift upon introduction of alkoxide ligands (300-500 ppm per alkoxide ligand) is consistent with what was observed for the Ti molecular systems and the corresponding V-based ZN pre-catalysts,[33] the isotropic chemical shift of all model systems based on the (110)-facet significantly diverged from the experimentally observed value ($\delta_{iso,\,exp}$ = –170 ppm), pointing out that this (crystalline) model does not capture the electronic structure of Ti sufficiently. Furthermore, these model systems do not reproduce the rather low C_Q value of the measured Ti species observed for the ZN pre-catalyst ($C_{Q,\,exp}$ = 9.3 MHz) well. The specific difference between experimental and computational values, in particular in terms of C_Q, indicates that Ti has to be in a more symmetrical environment than predicted from crystalline $MgCl_2$ models, paralleling what has been recently proposed for the corresponding V-based Ziegler-Natta pre-catalysts. In the latter case, the NMR response is in better agreement when $MgCl_2$ is modeled by a disordered model (nanoribbon) rather than crystalline (110)-facet models. It is noteworthy that the metal sites adopt a more symmetric environment when adsorbed on nanoribbon, whereby the fully chlorinated Ti site ($TiCl_4$@$MgCl_2$-NR) is associated with a calculated chemical shift and C_Q value of –122 ppm and 11.7 MHz, respectively. Such calculated values show similar trends upon substituting Cl by OR ligands, namely increasing shielding and C_Q values, and match within the level of uncertainty the experimental values (–170 ppm and 9.3 MHz). Overall, these results indicate that the ZN pre-catalysts treated with BCl_3 contain a well-defined Ti surface site, best described as being fully chlorinated and having a more symmetric environment inherited from being absorbed on disordered $MgCl_2$ (see Fig. 1 and 2).

This data also indicates that it is currently only possible to observe $^{47/49}$Ti NMR signatures when Ti is solely decorated by Cl ligands as in the BCl_3-treated ZN pre-catalyst, because of the associated lower C_Q and thereby narrow lines. On the contrary, the untreated ZN pre-catalysts, that has been shown to contain Ti-alkoxy species by ^{13}C NMR, is expected to contain Ti sites with (extremely) large C_Q leading to significant second-order quadrupolar line broadening, which would be currently impossible to observe with the state-of-the-art equipment even at prolonged measurement times.[21]

We next examined the orientation of the chemical shielding tensor (CST) and carried out a Natural Chemical Shielding (NCS)[50-53] analysis of the surface Ti sites in $TiCl_{4-x}(OR)_x$@$MgCl_2$-NR with the goal to rationalize the chemical shift trends observed upon substitution of Cl for OR ligands (detailed analysis of $TiCl_{4-x}(OR)_x$@$MgCl_2$-110-facet in ESI). Notably, the CST orientation strongly depends on the symmetry of the system and the number of terminal Cl/OR ligands. For the fully chlorinated system, $TiCl_4$@$MgCl_2$-NR, the most deshielded component (σ_{11}/δ_{11}) is oriented perpendicular to the plane containing Ti and the two terminal *cis*-Cl ligands (μ_1-Cl), associated with short Ti-Cl bonds (Fig. 3a), with σ_{22} bisecting the μ_1-Cl–Ti–μ_1-Cl angle, and σ_{33} being perpendicular to the other two components. With one terminal alkoxide ligand, as in $TiCl_3OR$@$MgCl_2$-NR, σ_{11} is oriented along the Ti-OR bond, while σ_{22} is oriented perpendicular to the plane containing Ti and the terminal Cl and OR ligands. When both terminal ligands are alkoxides ($TiCl_2(OR)_2$@$MgCl_2$-NR), the CST adopts a similar orientation as in the fully chlorinated system. Noteworthy, the chemical shift across the series of model systems is significantly influenced by the CST component perpendicular to the plane containing Ti and the two terminal μ_1-X (Cl/OR) ligands. The subsequent NCS analysis shows that

https://doi.org/10.26434/chemrxiv-2023-2hmzj-v2 **ORCID:** https://orcid.org/0000-0002-8624-1002 Content not peer-reviewed by ChemRxiv. **License:** CC BY-NC-ND 4.0

the chemical shift is mostly driven by the paramagnetic part of the chemical shifts and thereby the nature and the relative energies of high-lying occupied and low-lying unoccupied molecular orbitals, as evidenced by the Ramsey equation (Fig. 3d). The NCS analysis reveals that the chemical shift originates predominantly from the coupling between the σ(Ti-μ_1-X) and π*(Ti-μ_1-X) orbitals, as well as to a smaller extent the corresponding π(Ti-μ_1-X) and σ*(Ti-μ_1-X) orbitals (see ESI). The introduction of more electronegative terminal alkoxide ligands results in a larger energy gap between the coupled σ and π* orbitals and consequently to a smaller deshielding as expected from the Ramsey equation[54] (see Fig. 3d).

Conclusion

Overall, we have established a protocol to measure and calculate the $^{47/49}$Ti NMR spectroscopic signatures for Ti surface sites, focusing here on an industrially relevant ZN pre-catalysts based on $TiCl_4$ adsorbed on $MgCl_2$. We have found that the $^{47/49}$Ti NMR signatures are highly sensitive to the presence of alkoxides bound to Ti and to the local coordination environment imposed by the morphology of $MgCl_2$ support. Notably, employing DFS-QCPMG MAS NMR at 21.1 T and 100 K a single $^{47/49}$Ti NMR signature with a chemical shift of -170 ppm and a low C_Q of 9.3 MHz is observed in the ZN pre-catalyst treated with BCl_3, that indicates the presence of a well-defined species with a rather symmetric environment, best described as a hexacoordinated Ti species adsorbed on a disordered $MgCl_2$ with only chlorido ligands. We propose that the formation of these well-defined Ti sites results from the minimization of the charge distribution around Ti, only possible upon distortion of the Ti sites on the highly flexible ionic disordered $MgCl_2$ support (model here using the nanoribbon-like structure).

Observing the structure of this surface species indicates the role of BCl_3 and the support, and its overall well-defined structure is particularly noteworthy considering that ZN catalysts are multisite polymerization catalysts, possibly pointing that the multi-sites activity in these systems could be related to the activation steps with alkyl aluminium and transfer reactions rather than the complexity of the adsorbed Ti species on $MgCl_2$. We are currently exploring the matter in more details.

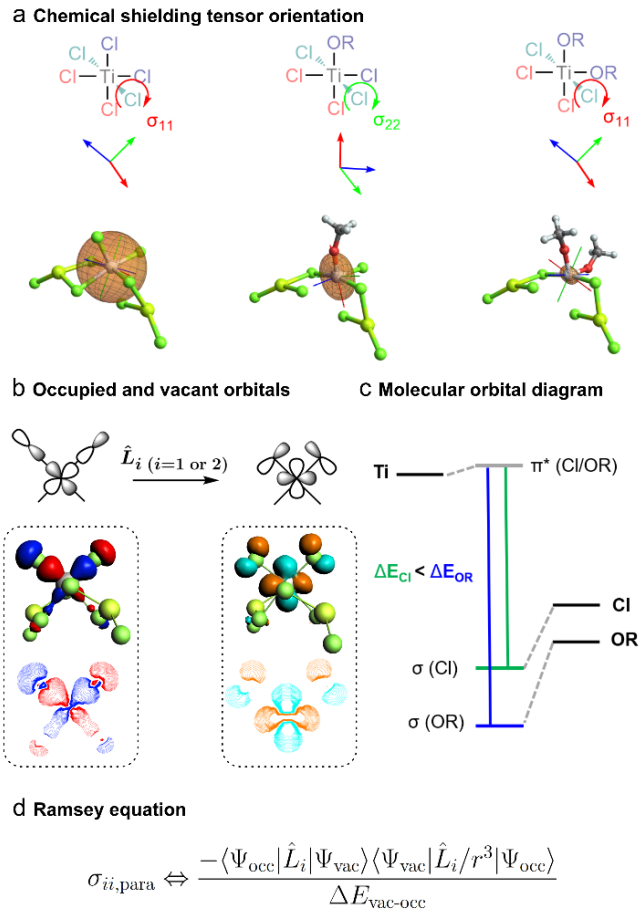

FIGURE 3. (a) Coordination environment of the Ti species with three distinct Cl ligands for $TiCl_4$@$MgCl_2$-NR (terminal: violet, *cis* to both terminal ligands: turquois, *trans* to one terminal ligand: red). Chemical shielding tensor orientation in the $TiCl_{4-x}(OR)_x$@$MgCl_2$-NR model systems (σ_{11} in red, σ_{22} in green and σ_{33} in blue).[55,56] (b) Rationalisation of the chemical shielding through the visualisation of the corresponding σ - π* Kohn-Sham orbitals obtained from the DFT calculations of the fully chlorinated ($TiCl_4$@$MgCl_2$-NR) surface model, which were selected by reconstruction of the Natural Localized Molecular Orbitals (NLMO) orbitals that contribute the most to the deshielding (see ESI). (c) The influence on the MO scheme upon exchanging the terminal ligands rationalizes the large deshielding for the fully chlorinated species compared to alkoxide species. (d) The Ramsey equation describes the chemical shielding arising from the magnetic coupling of occupied (ψ_{occ}) and vacant (ψ_{vac}) orbitals with an associated energy difference $\Delta E_{vac\text{-}occ}$ between these orbitals.[54]

https://doi.org/10.26434/chemrxiv-2023-2hmzj-v2 **ORCID:** https://orcid.org/0000-0002-8624-1002 Content not peer-reviewed by ChemRxiv. **License:** CC BY-NC-ND 4.0

ASSOCIATED CONTENT

Supporting Information. Synthesis protocols and corresponding solution NMR, single-crystal XRD structures, solid-state NMR measurement parameters and additional spectra, DFT calculation protocol for NMR parameters.

AUTHOR INFORMATION

Corresponding Author

*Alexander Yakimov
yakimov@inorg.chem.ethz.ch

*Christophe Copéret
ccoperet@ethz.ch

‡These authors contributed equally.

ACKNOWLEDGMENT

The authors thank Lyndon Emsley and Laura Piveteau for granting access to the 900 MHz LT NMR spectrometer at EPFL. The Euler supercomputer cluster is gratefully acknowledged for providing computational time. We are grateful to Dr. Matthieu Humbert and Dr. David Gajan (CRMN lab, UMR 5082) for fruitful discussions regarding ^{13}C CP-MAS spectroscopy.

Funding Sources

C.J. Kaul thanks the Swiss National Science Foundation (SNF IZLCZ0_206049) for financial support. Y. K. is grateful to the Swiss National Foundation (SNF) for financial support of this work (grant no. 200020B_192050). This project was partially funded through the ETH+ Project SynthMatLab. F. M. B. thanks the University of Lyon for funding his PhD.

REFERENCES

(1) Ziegler K., H. E., Breil H., Martin H. Das Mülheimer Normaldruck-Polyäthylen-Verfahren. *Angew. Chem.*, **1955**, *67*, 541-547.

(2) Natta, G. Une Nouvelle Classe de Polymeres d'α-Olefines ayant une Régularité de Structure Exceptionnelle. *J. Polym. Sci., Part A: Polym. Chem.,* **1996**, *34*, 321-332.

(3) Natta, G.; Pino, P.; Corradini, P.; Danusso, F.; Mantica, E.; Mazzanti, G.; Moraglio, G. CRYSTALLINE HIGH POLYMERS OF α-OLEFINS. *J. Am. Chem. Soc.,* **1955**, *77*, 1708-1710.

(4) Claverie, J. P.; Schaper, F. Ziegler-Natta catalysis: 50 years after the Nobel Prize. *MRS Bull.,* **2013**, *38*, 213-218.

(5) Kashiwa, N. The discovery and progress of $MgCl_2$-supported $TiCl_4$ catalysts. *J. Polym. Sci., Part A: Polym. Chem.,* **2004**, *42*, 1-8.

(6) Moore, E. P. (Ed.) Polypropylene handbook polymerization, characterization, properties, processing, applications; Hanser Publishers; Hanser Publishers: Munich, Germany. **1996**, 419 p.

(7) Piovano, A.; Signorile, M.; Braglia, L.; Torelli, P.; Martini, A.; Wada, T.; Takasao, G.; Taniike, T.; Groppo, E. Electronic Properties of Ti Sites in Ziegler–Natta Catalysts. *ACS Catal.,* **2021**, *11*, 9949-9961.

(8) Magni, E.; Somorjai, G. A. Preparation of a model Ziegler-Natta catalyst: electron irradiation induced titanium chloride deposition on magnesium chloride thin films grown on gold. *Surf. Sci.,* **1996**, *345*, 1-16.

(9) Mori, H.; Sawada, M.; Higuchi, T.; Hasebe, K.; Otsuka, N.; Terano, M. Direct observation of $MgCl_2$-supported Ziegler catalysts by high resolution transmission electron microscopy. *Macromol, Rapid Commun.,* **1999**, *20*, 245-250.

(10) Fregonese, D.; Glisenti, A.; Mortara, S.; Rizzi, G. A.; Tondello, E.; Bresadola, S. $MgCl_2/TiCl_4/AlEt_3$ catalytic system for olefin polymerisation: a XPS study. *J. Mol. Catal. A: Chem.,* **2002**, *178*, 115-123.

(11) Schmidt, J.; Risse, T.; Hamann, H.; Freund, H. J. Characterization of a model Ziegler–Natta catalyst for ethylene polymerization. *J. Chem. Phys.,* **2002**, *116*, 10861-10868.

(12) Kim, S. H.; Somorjai, G. A. Surface science of single-site heterogeneous olefin polymerization catalysts. *Proc. Natl. Acad. Sci. U.S.A.,* **2006**, *103*, 15289-15294.

(13) Andoni, A.; Chadwick, J. C.; Niemantsverdriet, H. J. W.; Thüne, P. C. A Preparation Method for Well-Defined Crystallites of $MgCl_2$-Supported Ziegler-Natta Catalysts and their Observation by AFM and SEM. *Macromol. Rapid Commun.,* **2007**, *28*, 1466-1471.

(14) Groppo, E.; Seenivasan, K.; Barzan, C. The potential of spectroscopic methods applied to heterogeneous catalysts for olefin polymerization. *Catal. Sci. Technol.,* **2013**, 858-878.

(15) Yakimov, A. V.; Mance, D.; Searles, K.; Copéret, C. A Formulation Protocol with Pyridine to Enable Dynamic Nuclear Polarization Surface-Enhanced NMR Spectroscopy on Reactive Surface Sites: Case Study with Olefin Polymerization and Metathesis Catalysts. *J. Phys. Chem. Lett.,* **2020**, *11*, 3401-3407.

(16) Yakimov, A.; Xu, J.; Searles, K.; Liao, W.-C.; Antinucci, G.; Friederichs, N.; Busico, V.; Copéret, C. DNP-SENS Formulation Protocols To Study Surface Sites in Ziegler–Natta Catalyst $MgCl_2$ Supports Modified with Internal Donors. *J. Phys. Chem. C,* **2021**, *125*, 15994-16003.

(17) Ashuiev, A.; Humbert, M.; Norsic, S.; Blahut, J.; Gajan, D.; Searles, K.; Klose, D.; Lesage, A.; Pintacuda, G.; Raynaud, J.; et al. Spectroscopic Signature and Structure of the Active Sites in Ziegler–Natta Polymerization Catalysts Revealed by Electron Paramagnetic Resonance. *J. Am. Chem. Soc.,* **2021**, *143*, 9791-9797.

(18) Albizzati, E.; Morini, G.; Giannini, U.; Barino, L.; Scordamaglia, R.; Barbe, C.; Noristi, L. Components and catalysts for the polymerization of olefins. CA2039443A1, **1991**.

(19) Wada, T.; Takasao, G.; Piovano, A.; D'Amore, M.; Thakur, A.; Chammingkwan, P.; Bruzzese, P. C.; Terano, M.; Civalleri, B.; Bordiga, S.; et al. Revisiting the identity of δ-$MgCl_2$: Part I. Structural disorder studied by synchrotron X-ray total scattering. *Journal of Catalysis* **2020**, *385*, 76-86.

(20) Zarupski, J.; Piovano, A.; Signorile, M.; Amodio, A.; Olivi, L.; Hendriksen, C.; Friederichs, N. H.; Groppo, E. Silica-Magnesium-Titanium Ziegler-Natta Catalysts. Part I: Structure of the Pre-Catalyst at a Molecular Level. Part I: Structure of the Pre-Catalyst at a Molecular Level. *J. Catal.*, **2023**, *424*, 236-245.

https://doi.org/10.26434/chemrxiv-2023-2hmzj-v2 **ORCID:** https://orcid.org/0000-0002-8624-1002 Content not peer-reviewed by ChemRxiv. **License:** CC BY-NC-ND 4.0

(21) Blaakmeer, E. S. M.; Antinucci, G.; Correa, A.; Busico, V.; van Eck, E. R. H.; Kentgens, A. P. M. Structural Characterization of Electron Donors in Ziegler–Natta Catalysts. *J. Phys., Chem., C,* **2018**, *122*, 5525-5536.

(22) Blaakmeer, E. S. M.; Antinucci, G.; van Eck, E. R. H.; Kentgens, A. P. M. Probing Interactions between Electron Donors and the Support in $MgCl_2$-Supported Ziegler–Natta Catalysts. *J. Phys. Chem. C,* **2018**, *122*, 17865-17881.

(23) Tijssen, K. C. H.; Blaakmeer, E. S.; Kentgens, A. P. M. Solid-state NMR studies of Ziegler–Natta and metallocene catalysts. *Solid State Nucl. Magn. Reson.,* **2015**, *68-69*, 37-56.

(24) Blaakmeer, E. S.; Antinucci, G.; Busico, V.; van Eck, E. R. H.; Kentgens, A. P. M. Solid-State NMR Investigations of $MgCl_2$ Catalyst Support. *J. Phys. Chem. C,* **2016**, *120*, 6063-6074.

(25) Blaakmeer, E. S.; van Eck, E. R. H.; Kentgens, A. P. M. The coordinative state of aluminium alkyls in Ziegler–Natta catalysts. *Phys. Chem. Chem. Phys.,* **2018**, *20*, 7974-7988.

(26) Grau, E.; Lesage, A.; Norsic, S.; Copéret, C.; Monteil, V.; Sautet, P. Tetrahydrofuran in $TiCl_4$/THF/$MgCl_2$: a Non-Innocent Ligand for Supported Ziegler–Natta Polymerization Catalysts. *ACS Catal.,* **2013**, *3*, 52-56.

(27) D'Anna, V.; Norsic, S.; Gajan, D.; Sanders, K.; Pell, A. J.; Lesage, A.; Monteil, V.; Copéret, C.; Pintacuda, G.; Sautet, P. Structural Characterization of the EtOH–$TiCl_4$–$MgCl_2$ Ziegler–Natta Precatalyst. *J. Phys. Chem. C,* **2016**, *120*, 18075-18087.

(28) Humbert, M.; Norsic, S.; Raynaud, J.; Monteil, V. Activity Enhancement of $MgCl_2$-supported Ziegler-Natta Catalysts by Lewis-acid Pre-treatment for Ethylene Polymerization. *Chin. J. Polym. Sci.,* **2019**, *37*, 1031-1038.

(29) Stone, N. J. Table of nuclear electric quadrupole moments. *At. Data Nucl. Data Tables,* **2016**, *111-112*, 1-28.

(30) Lucier, B. E. G.; Huang, Y. Chapter One - Reviewing $^{47/49}$Ti Solid-State NMR Spectroscopy: From Alloys and Simple Compounds to Catalysts and Porous Materials. In *Annu. Rep. NMR Spectrosc.*, Webb, G. A. Ed.; Vol. 88; Academic Press, **2016**; pp 1-78.

(31) Blaakmeer, E. S.; Wensink, F. J.; van Eck, E. R. H.; de Wijs, G. A.; Kentgens, A. P. M. Preactive Site in Ziegler–Natta Catalysts. *J. Phys. Chem. C,* **2019**, *123*, 14490-14500.

(32) Lätsch, L.; Kaul, C., Yakimov, A. V.,; Müller, I.B., Hassan, A.; Perrone, B., Aghazada, S.; Berkson, Z. J.; De Baerdemaeker, T.; Parvulescu, A.-N.; Seidel, K.; Teles, J. H.; Copéret C. NMR Signatures and Electronic Structure of Ti Sites in Titanosilicalite-1 from Solid-State $^{47/49}$Ti NMR Spectroscopy. **2023**, 145, 15018-15023.

(33) Sabisch S., Kakiuchi Y., Docherty S.R., Yakimov A., Copéret C. Geometry and local environment of surface sites in Vanadium-based Ziegler-Natta catalysts from ^{51}V solid-state NMR Spectroscopy. *ChemRxiv* **2023**. DOI: 10.26434/chemrxiv-2023-f59zx-v2 (2023-09-07).

(34) Rannabauer, S.; Schnick, W. Synthese, Kristallstruktur und spektroskopische Charakterisierung von Bis(dimethylammonium)hexachlorotitanat $[Me_2NH_2]_2[TiCl_6]$/ Synthesis, Crystal Structure, and Spectroscopic Characterization of Bis(dimethylammonium) Hexachlorotitanate $[Me_2NH_2]_2[TiCl_6]$. *Z. Naturforsch. B.* **2003**, *58*, 410-414.

(35) Larsen, F.H.; Jakobsen, H.J.; Ellis, P.D.; Nielsen, N.C. QCPMG-MAS NMR of Half-Integer Quadrupolar Nuclei. *J. Magn. Reson.* **1998**, *131*, 144-147.

(36) Iuga, D.; Schäfer, H.; Verhagen, R.; Kentgens, A.P.M. Population and Coherence Transfer Induced by Double Frequency Sweeps in Half-Integer Quadrupolar Spin Systems. *J. Magn. Reson.* **2000**, *147*, 192-209.

(37) te Velde, G.; Bickelhaupt, F.M.; Baerends, E.J.; Fonseca Guerra, C.; van Gisbergen, S.J.A.; Snijders, J.G.; Ziegler, T. Chemistry with ADF. *J. Comput. Chem.* **2001**, *22*, 931-967.

(38) Becke, A.D. Density-functional thermochemistry. III. The role of exact exchange. *J. Chem. Phys.* **1993**, *98*, 5648-5652.

(39) Stephens, P.J.; Devlin, F.J.; Chabalowski, C.F.; Frisch, M.J. Ab Initio Calculation of Vibrational Absorption and Circular Dichroism Spectra Using Density Functional Force Fields. *J. Phys. Chem.* **1994**, *98*, 11623-11627.

(40) Van Lenthe, E.; Baerends, E. J. Optimized Slater-type basis sets for the elements 1–118. *J. Comput. Chem.* **2003**, *24*, 1142-1156.

(41) Wolff, S.K.; Ziegler, T.; van Lenthe, E.; Baerends, E.J. Density functional calculations of nuclear magnetic shieldings using the zeroth-order regular approximation (ZORA) for relativistic effects: ZORA nuclear magnetic resonance. *J. Chem. Phys.* **1999**, *110*, 7689-7698.

(42) Hao, N.; Sayer, B.G.; Dénès, G.; Bickley, D.G.; Detellier, C.; McGlinchey, M.J. Titanium-47 and -49 nuclear magnetic resonance spectroscopy: Chemical applications. *J. Magn. Reson.* **1982**, *50*, 50-63.

(43) Berger, S.; Bock, W.; Marth, C. F.; Raguse, B.; Reetz, M. T. $^{47/49}$Ti NMR of some titanium compounds. *Magn. Reson. Chem.* **1990**, *28*, 559-560.

(44) Berger, S.; Bock, W.; Frenking, G.; Jonas, V.; Mueller, F. NMR Data of Methyltitanium Trichloride and Related Organometallic Compounds. A Combined Experimental and Theoretical Study of $MenXCl_{4-n}$ (n = 0-4; X = C, Si, Sn, Pb, Ti). *J. Am. Chem. Soc.* **1995**, *117*, 3820-3829.

(45) Correa, A.; Credendino, R.; Pater, J.T.M.; Morini, G.; Cavallo, L. Theoretical Investigation of Active Sites at the Corners of $MgCl_2$ Crystallites in Supported Ziegler–Natta Catalysts. *Macromolecules,* **2012**, *45*, 3695-3701.

(46) Breuza, E.; Antinucci, G.; Budzelaar, P.H.M.; Busico, V.; Correa, A.; Ehm, C. $MgCl_2$-Supported Ziegler–Natta Catalysts: a DFT-D "Flexible-Cluster" Approach to Internal Donor Adducts. *J. Phys. Chem. C,* **2018**, *122*, 9046-9053.

(47) D'Amore, M.; Thushara, K.S.; Piovano, A.; Causà, M.; Bordiga, S.; Groppo, E. Surface Investigation and Morphological Analysis of Structurally Disordered $MgCl_2$ and $MgCl_2$/$TiCl_4$ Ziegler–Natta Catalysts. *ACS Catal.,* **2016**, *6*, 5786-5796.

(48) Seth, M.; Margl, P.M.; Ziegler, T.A Density Functional Embedded Cluster Study of Proposed Active Sites in Heterogeneous Ziegler–Natta Catalysts. *Macromolecules,* **2002**, *35*, 7815-7829.

(49) Correa, A.; Piemontesi, F.; Morini, G.; Cavallo, L. Key Elements in the Structure and Function Relationship of the $MgCl_2$/$TiCl_4$/Lewis Base Ziegler–Natta Catalytic System. *Macromolecules,* **2007**, *40*, 9181-9189.

(50) Autschbach, J.; Zheng, S. Analyzing Pt chemical shifts calculated from relativistic density functional theory using localized orbitals: The role of Pt 5d lone pairs. *Magn. Reson. Chem.,* **2008**, *46*, S45-S55.

(51) Widdifield, C.M.; Schurko, R.W. Understanding chemical shielding tensors using group theory, MO analysis, and modern density-functional theory. *Concepts Magn. Reson., Part A,* **2009**, *34A*, 91-123.

(52) Gordon, C.P.; Lätsch, L.; Copéret, C. Nuclear Magnetic Resonance: A Spectroscopic Probe to Understand the Electronic Structure and Reactivity of Molecules and Materials. *J. Phys. Chem. Lett.,* **2021**, *12*, 2072-2085.

(53) Nater, D.F.; Kaul, C.J.; Lätsch, L.; Tsurugi, H.; Mashima, K.; Copéret, C. Olefin Metathesis Catalysts Generated In Situ from Molybdenum(VI)-Oxo Complexes by Tuning Pendant Ligands. *Chem. Eur. J.,* **2022**, *28*, e202200559.

(54) Ramsey, N.F. Magnetic Shielding of Nuclei in Molecules. *Phys. Rev.,* **1950**, *78*, 699-703.

(55) Zurek, E.; Pickard, C.J.; Autschbach, J. Density Functional Study of the 13C NMR Chemical Shifts in Single-Walled Carbon Nanotubes with Stone–Wales Defects. *J. Phys. Chem. C,* **2008**, *112*, 11744-11750.

https://doi.org/10.26434/chemrxiv-2023-2hmzj-v2 **ORCID:** https://orcid.org/0000-0002-8624-1002 Content not peer-reviewed by ChemRxiv. **License:** CC BY-NC-ND 4.0

(56) Autschbach, J.; Zheng, S.; Schurko, R.W. Analysis of electric field gradient tensors at quadrupolar nuclei in common structural motifs. *Concepts Magn. Reson., Part A,* **2010**, *36A*, 84-126.

https://doi.org/10.26434/chemrxiv-2023-2hmzj-v2 **ORCID:** https://orcid.org/0000-0002-8624-1002 Content not peer-reviewed by ChemRxiv. **License:** CC BY-NC-ND 4.0

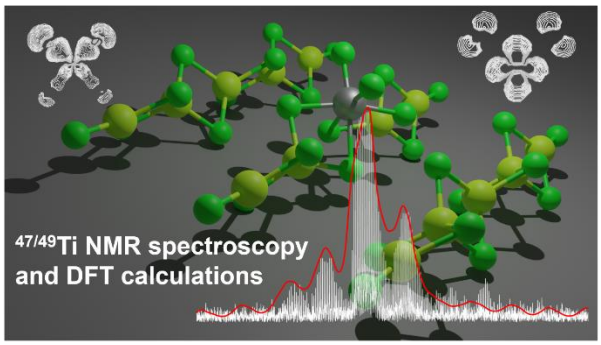

https://doi.org/10.26434/chemrxiv-2023-2hmzj-v2 **ORCID:** https://orcid.org/0000-0002-8624-1002 Content not peer-reviewed by ChemRxiv. **License:** CC BY-NC-ND 4.0